

Partitioning and Conformational Behavior of Polyelectrolytes Confined in a Cylindrical Pore

Pyeong Jun Park, Myung-Suk Chun,* and Jae-Jin Kim

Biomaterials Research Center, Korea Institute of Science and Technology, PO Box 131, Cheongryang, Seoul 130–650, South Korea

Received January 3, 2000; Revised Manuscript Received August 28, 2000

ABSTRACT: We study the behavior of a uniformly charged polyelectrolyte confined in a circular cylindrical pore with constant surface potentials. From Green's function theory with an effective step-length renormalized by monomer–monomer interactions, the partition coefficient and associated chain conformations are predicted in a variety of situations. Depending upon the ionic strength of surrounding fluids, the polyelectrolyte conformation may be stretched and follow a self-avoiding walk, yielding a significant reduction in the partition coefficient compared to the ideal chain result. The monomer–monomer interaction is found to be as important as the polymer–pore interaction in determining the partitioning behavior, especially in the long-chain regime, due to the characteristics of confined spaces.

I. Introduction

Polymers in confined spaces have been the subject of much interest,¹ not only because they are interesting theoretically but also because there are many practical applications such as membrane filtration, size exclusion chromatography, and DNA gel electrophoresis. The primary factor governing the conformational properties of polymers in confined spaces is the reduced chain entropy due to the steric repulsion of the wall.² When the polymer repulsively interacts with the wall, the chain statistical weight can be further reduced since the repulsion may bring about a stronger chain confinement by forming a depletion layer near the wall. On the other hand, a competing mechanism may exist if the confining wall attractively interacts with the chain molecules. The attraction effectively cancels the steric repulsion at the adsorption–desorption threshold, beyond which the chain prefers being localized near the attracting wall. Therefore, the long-range polymer–pore interaction, whether repulsive or attractive, should be no less important than the short-range steric polymer–pore interaction in determining the statistical weight of polymers confined in a pore.^{3,4}

Because of the strong coupling between the conformation and dynamics of polymers,⁵ the polymer–pore interaction plays an important role also in the dynamics of polymers in confined spaces.⁶ While the hindered diffusion of finite-sized colloidal particles in confined spaces has been extensively studied,⁷ understanding the diffusion of polymers in random or regular confining geometries is still in a primitive stage.^{8,9} In general, the chain transport coefficient is given by the partition coefficient times the hindrance factor arising from the hydrodynamic interaction between the chain and the wall.⁷ It is therefore essential to know the partition coefficient as well as the associated chain conformation to study the hindered diffusion of polymers in confined spaces.

Unlike the partitioning of colloids into confined spaces, where rigorous studies have been performed,^{7,10} partitioning of polymers has been investigated only in

a few limited situations.¹ Casassa derived an analytical expression for the steric partition coefficient of an ideal chain, which emphasizes the chain entropy reduction due to confinements.¹¹ Using the scaling theory, Daoud and de Gennes studied the effects of excluded volume interaction.¹² Deen and co-workers numerically solved the diffusion-type equation and studied the polyelectrolyte partitioning into a spherical cavity³ as well as into a cylindrical pore.⁴ Their investigation was successful in illustrating the role of polymer–pore interactions, yet the effects of intramolecular interactions as well as the associated chain conformations remain in question. More rigorous approaches have been employed recently to study the behavior of polyelectrolytes interacting with charged flat surfaces,¹³ emphasizing the effects of charge distribution along the chain contour. Experimental works on the partitioning of flexible polymers have been provided,^{14–16} focusing on the effects of molecular weights, excluded volume interactions, and polymer–pore steric interactions. For the steric partition coefficient, theoretical predictions with or without the excluded volume effect were confirmed,^{14,15} but pertinent experiments regarding the effects of polymer–pore interactions as well as intramolecular interactions should be performed.

In this paper, we address the problem of polyelectrolytes partitioning into a circular cylindrical pore filled with ionic solutions. Especially, we focus on the effects of screened electrostatic interactions and excluded volume interactions between monomers and the pore wall as well as between pairs of monomers. Since the problem inherently includes many body interaction between pairs of monomers, a Gaussian chain theory is used with an effective segmental length renormalized by the intramolecular interactions, which is originally suggested by Muthukumar.¹⁷ By adapting this effective step-length description, we reduce the problem to a familiar Schrödinger problem with external potentials, and then apply the standard perturbation theory and a variational theory depending upon the polymer–pore interaction parameters. We neglect the counterion effects and determine the electrostatic potential within the pore by using the Debye–Hückel approximation. Therefore, our results are strictly valid when the

* Corresponding author. E-mail: mschun@kist.re.kr.

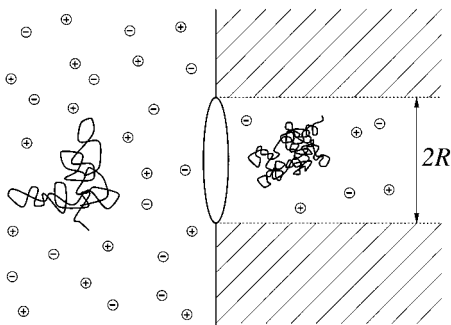


Figure 1. Schematic view of a polyelectrolyte partitioning into a cylindrical pore. The pore wall is maintained with fixed electrostatic potential, and the ions are floating around.

polyelectrolyte has a low charge density and the pore wall is maintained with a small electrostatic potential. As the main results, partition coefficients of polyelectrolytes are presented in a variety of situations, and the associated chain conformational properties are discussed in terms of the monomer distribution function and the polymer radius of gyration.

This paper is organized as follows. In section II, the partition coefficient of polyelectrolytes is defined, and results for a limiting situation are discussed. In section III, the effective step-length description is introduced, and the steric partition coefficient is calculated. In section IV, the weakly screened electrostatic interaction regime is examined using the first-order perturbation theory. In section V, effects of the strongly screened interaction are investigated using a variational theory. Finally, a summary is given in section VI.

II. Definition of the Partition Coefficient

Consider a dilute solution of uniformly charged polyelectrolytes exposed to a cylindrical pore as shown in Figure 1. The polymers would prefer either being situated within the pore or being situated in the bulk solution, depending upon its radius of gyration, its interaction with the pore wall, and the screening effect. As a measure of this preference, we define the partition coefficient of a polymer as

$$K = \exp(-F/k_B T) \quad (1)$$

where $k_B T$ is the thermal energy and F is the free energy required for a polymer to be inserted into the pore from the bulk solution. In case that there exists only the steric interaction between the polymer and the pore wall, the partition coefficient may be reduced to

$$K = \exp(\Delta S/k_B) \quad (2)$$

where ΔS is the entropy reduction due to the confinement of the pore. The partition coefficient K is the probability of finding a polymer in the pore, which can also be interpreted as the ratio of equilibrium concentrations in the pore and in the bulk solution.

To study the partitioning behavior of polyelectrolytes, one has to know the electrostatic potential function within the pore. We use the Debye–Hückel approximation for the electrostatic potential $\phi(r)$ in a sufficiently long circular cylindrical pore with radius R . Then $\phi(r)$ satisfies

$$\nabla^2 \phi = \kappa^2 \phi \quad (3)$$

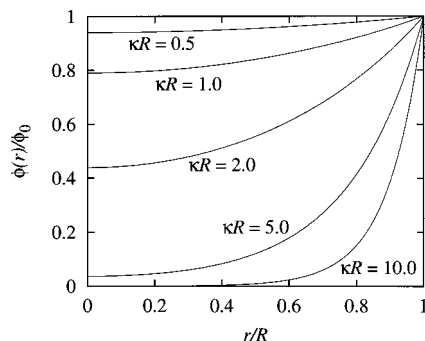


Figure 2. Electrostatic potential inside the cylindrical pore for various values of κR .

where κ is the inverse Debye screening length defined by

$$\kappa^2 = \frac{2Z^2 \rho_0}{k_B T} \quad (4)$$

Here Z is the valency of the ions in the surrounding fluids, and ρ_0 is the electrolyte concentration. Throughout this paper, we set the elementary charge and the dielectric constant of the ionic solution equal to unity. The solution of eq 3 in cylindrical coordinates is given by

$$\phi(r) = \phi_0 \frac{I_0(\kappa r)}{I_0(\kappa R)} \quad (5)$$

where ϕ_0 is the constant electrostatic potential on the pore wall at $r = R$ and $I_0(x)$ is the modified Bessel function of the first kind of order zero. In Figure 2, the potential function is plotted for several values of κR . When $\kappa \rightarrow 0$, the potential $\phi(r)$ has a constant value ϕ_0 everywhere within the pore. On the other hand, when κR has a nonvanishing value, the screening effect turns on and develops a double layer with thickness κ^{-1} from the pore wall.

Let us now consider a limiting situation that the polymer coil size is much smaller than the pore radius R and the Debye length κ^{-1} . In this case, the polymer–pore interaction hardly affects the polymer conformation, so that the polymer can be assumed to be a colloidal particle. We set the total charge of the polymer equal to $L\sigma$, with L the polymer contour length and σ the charge density along the contour. Then the partition coefficient can be written as

$$K \approx \frac{2}{R^2} \int_0^R e^{-\beta \sigma L \phi(r)} r \, dr \quad (6)$$

where $\beta = 1/k_B T$. By numerically integrating this expression, one can obtain the partition coefficient as shown in Figure 3. As expected, the partition coefficient decreases as $\beta \sigma L \phi_0$ increases. Note also that the screening effect appears when κR becomes larger than unity. An analytic expression for the partition coefficient is available in the weak ionic strength regime ($\kappa R \lesssim 1$). Using an approximate expression for the potential

$$\phi(r) \approx \phi_0 \left[1 + \frac{1}{4} \kappa^2 (r^2 - R^2) \right] \quad (7)$$

one can calculate the partition coefficient from eq 6 as

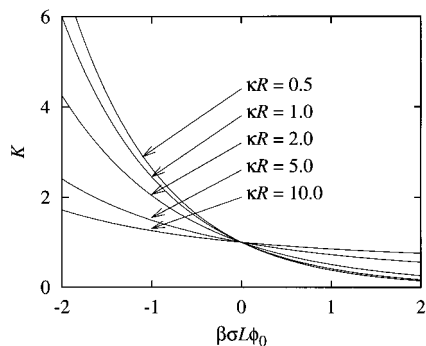


Figure 3. Partition coefficient K of a polyelectrolyte in the small radius of gyration limit. K is identical to the partition coefficient of a colloidal particle with charge σL .

$$K \approx \exp(-\beta\sigma L\phi_0) \left[\frac{e^\mu \sinh \mu}{\mu} \right] \quad (8)$$

where $\mu \equiv (\kappa^2 R^2/8)\beta\sigma L\phi_0$. The results in this colloidal particle limit will serve as a reference that can be compared to the more complex situations to be discussed below.

III. Statistical Mechanics of a Polyelectrolyte Confined in a Pore: The Steric Partition Coefficient

The Green's function $G_L(\mathbf{r}, \mathbf{r}')$ of a polymer with its contour length L , defined as the probability of finding one end at \mathbf{r} when the other end is located at \mathbf{r}' , can be written in the functional integral form as follows:

$$G_L(\mathbf{r}, \mathbf{r}') = \int_{\mathbf{R}(0)=\mathbf{r}'}^{\mathbf{R}(L)=\mathbf{r}} D[\mathbf{R}(s)] \exp \left[-\frac{3}{2l} \int_0^L ds \left(\frac{\partial \mathbf{R}(s)}{\partial s} \right)^2 - \beta W[\mathbf{R}(s)] \right] \quad (9)$$

where l is the Kuhn length and $W[\mathbf{R}(s)]$ is the total interaction energy arising from the intramolecular interactions as well as from the polymer-pore interaction. We consider the interaction energy modeled as

$$\beta W[\mathbf{R}(s)] = \frac{w_c}{2} \int_0^L ds \int_0^L ds' \frac{e^{-\kappa|\mathbf{R}(s)-\mathbf{R}(s')|}}{|\mathbf{R}(s)-\mathbf{R}(s')|} + \frac{w}{2} \int_0^L ds \int_0^L ds' \delta(\mathbf{R}(s)-\mathbf{R}(s')) + \beta \int_0^L ds \mathcal{U}(\mathbf{R}(s)) \quad (10)$$

The first term is the screened electrostatic interaction between all pairs of the chain segments with $w_c = \beta\sigma^2 = l_B\sigma^2$, where l_B is the Bjerrum length. The second term is the short-range excluded volume interaction with

$$w = l^2 \int d\mathbf{r} (1 - e^{-\beta u(\mathbf{r})}) \quad (11)$$

where $u(\mathbf{r})$ is the potential energy due to the steric interaction between two monomers with distance vector \mathbf{r} . The last term in eq 10 represents the electrostatic interaction between the polymer and the pore wall. Here, $\mathcal{U}(\mathbf{R}(s)) ds$ is the potential energy of the chain segments from $\mathbf{R}(s)$ to $\mathbf{R}(s+ds)$ given by

$$\beta \mathcal{U}(\mathbf{R}(s)) = \beta\sigma\phi_0 \frac{I_0(\kappa r)}{I_0(\kappa R)} \quad (12)$$

where r is the radial distance of $\mathbf{R}(s)$ from the cylinder axis.

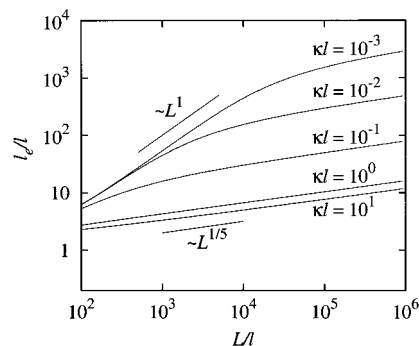


Figure 4. Effective step-length l_e as a function of chain contour length L for different values of κl ($w/l = 1$, and $w_c l = 0.1$).

Since the functional integral in eq 9 is difficult to handle due to the complicated potential energy, we follow the variational procedure suggested by Muthukumar.¹⁷ Considering the intramolecular interaction separately, the polyelectrolyte can be treated as an ideal chain with an effective step-length l_e instead of l . Then Green's function in eq 9 can be approximated as

$$G_L(\mathbf{r}, \mathbf{r}') \approx \int_{\mathbf{R}(0)=\mathbf{r}'}^{\mathbf{R}(L)=\mathbf{r}} D[\mathbf{R}(s)] \exp \left[-\frac{3}{2l_e} \int_0^L ds \left(\frac{\partial \mathbf{R}(s)}{\partial s} \right)^2 - \beta \int_0^L ds \mathcal{U}[\mathbf{R}(s)] \right] \quad (13)$$

In the above, the effective step-length l_e is given by¹⁷

$$l_e^{3/2} \left[\frac{1}{l} - \frac{1}{l_e} \right] = \zeta_{ev} + \zeta_c \quad (14)$$

where

$$\zeta_{ev} = \frac{4}{3} \left(\frac{3}{2\pi} \right)^{3/2} \frac{wL^{1/2}}{l_e} \quad (15)$$

$$\zeta_c = \frac{4}{45} \left(\frac{6}{\pi} \right)^{1/2} w_c L^{3/2} \left[\frac{15\pi^{1/2} e^a}{2a^{5/2}} (a^2 - 4a + 6) \operatorname{erfc}(a^{1/2}) - 15\sqrt{\pi} \left(\frac{3}{a^{5/2}} + \frac{1}{a^{3/2}} \right) + \frac{90}{a^2} \right] \quad (16)$$

with

$$a = \frac{1}{6} \kappa^2 L l_e \quad (17)$$

In eq 16, we corrected trivial errors in the original paper.¹⁷ The effective step-length obtained from the above formula is shown in Figure 4 for various values of κl . There appears a crossover from $l_e \sim L$ to $l_e \sim L^{1/5}$ at a chain length corresponding to $\kappa R_G \approx 1$, where $R_G = (Ll_e/6)^{1/2}$ is the polymer radius of gyration. This leads to the following behavior in R_G^2 :

$$R_G^2 = \frac{1}{6} L l_e \sim \begin{cases} L^2 & (\text{for } \kappa R_G \lesssim 1) \\ L^{6/5} & (\text{for } \kappa R_G \gtrsim 1) \end{cases} \quad (18)$$

which represents a crossover from stretched to self-avoiding chain regime.

The effective step-length description is a mean field approximation of intramolecular interactions. In this approach, the Gaussian chain conformation is assumed so that the external potential plays no role in determin-

ing the effective step-length. Despite the simplicity of this approximation, however, it gives correct results not only for the swelling exponents of a chain with intramolecular interactions¹⁷ but also for the chain adsorption characteristics in several applications.^{17,18} Throughout this paper we employ this effective step-length to incorporate the intramolecular interactions, referring to the literature for further details on this approximation.¹⁷

The differential equation for Green's function in eq 13 is given by

$$\left[\frac{\partial}{\partial L} - \frac{l_e}{6} \nabla^2 + \beta \mathcal{L}(\mathbf{r}) \right] G_L(\mathbf{r}, \mathbf{r}') = 0 \quad (19)$$

with an initial condition

$$\lim_{L \rightarrow 0} G_L(\mathbf{r}, \mathbf{r}') = \delta(\mathbf{r} - \mathbf{r}') \quad (20)$$

The Green's function can be expanded as

$$G_L(\mathbf{r}, \mathbf{r}') = \sum_n \exp(-L\lambda_n) \psi_n(\mathbf{r}) \psi_n(\mathbf{r}') \quad (21)$$

where $\{\lambda_n\}$ and $\{\psi_n(\mathbf{r})\}$ are the sets of eigenvalues and eigenfunctions, respectively, which can be obtained from

$$\left[-\frac{l_e}{6} \nabla^2 + \beta \mathcal{L}(\mathbf{r}) \right] \psi_n(\mathbf{r}) = \lambda_n \psi_n(\mathbf{r}) \quad (22)$$

We impose the normalization of $\psi_n(\mathbf{r})$ in such a way that

$$\int_V |\psi_n(\mathbf{r})|^2 d\mathbf{r} = 1 \quad (23)$$

where the integration is over the pore volume $V = \pi R^2 h$ with h the pore length. In terms of Green's function, the free energy of a polymer in a confinement relative to that in a bulk fluid can be written as

$$F = -k_B T \log \left[\frac{1}{V} \int_V d\mathbf{r} \int_V d\mathbf{r}' G_L(\mathbf{r}, \mathbf{r}') \right] \quad (24)$$

The monomer density distribution can also be obtained from Green's function as

$$\rho(\mathbf{r}) = \left[\int_V d\mathbf{r}' \int_V d\mathbf{r}'' \frac{1}{L} \int_0^L ds G_s(\mathbf{r}', \mathbf{r}) G_{L-s}(\mathbf{r}, \mathbf{r}') \right] / \left[\int_V d\mathbf{r}' \int_V d\mathbf{r}'' G_L(\mathbf{r}', \mathbf{r}'') \right] \quad (25)$$

with $\int_V \rho(\mathbf{r}) d\mathbf{r} = 1$.

Let us now consider the case of $\phi_0 = 0$ and calculate the steric partition coefficient of a polyelectrolyte chain. Since $\mathcal{L}(\mathbf{r}) = 0$, the relevant part of eq 22 in cylindrical coordinates becomes

$$-\frac{l_e}{6} \left[\frac{\partial^2}{\partial r^2} + \frac{1}{r} \frac{\partial}{\partial r} + \frac{1}{r^2} \frac{\partial^2}{\partial \theta^2} \right] \psi_{mn}(r, \theta) = \lambda_{mn} \psi_{mn}(r, \theta) \quad (26)$$

which yields

$$\lambda_{mn} = \frac{l_e}{6R^2} (\nu_{mn}^2 + m^2) \quad (27)$$

$$\psi_{mn} = \frac{1}{\pi^{1/2} R J_m(\nu_{mn})} J_m(\nu_{mn} r/R) e^{im\theta} \quad (28)$$

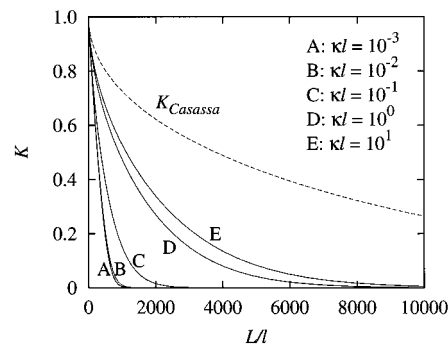


Figure 5. Partition coefficient with $\phi_0 = 0$ for different values of κl . The dotted line (K_{Casassa}) is Casassa's result for an ideal chain. Throughout this paper, the parameter values used are $R/l = 100$, $w/l = 1$, and $w_c l = 0.1$.

where ν_{mn} is the n th root of $J_m(x)$, the Bessel function of order m . In terms of these results, Green's function can be explicitly written as

$$G_L(\mathbf{r}, \mathbf{r}') = \left(\frac{2\pi L l_e}{3} \right)^{-1/2} e^{-3(z-z')^2/2Ll_e} \times \sum_{m,n} e^{-L\lambda_{mn}} \frac{J_m(\nu_{mn} r/R) J_m(\nu_{mn} r'/R) e^{im(\theta-\theta')}}{\pi R^2 [J_m(\nu_{mn})]^2} \quad (29)$$

By assuming $h \gg R_G$, we obtain the partition coefficient

$$\begin{aligned} K &= \frac{1}{V} \int_V d\mathbf{r} \int_V d\mathbf{r}' G_L(\mathbf{r}, \mathbf{r}') \\ &= 4 \sum_n \nu_{0n}^{-2} \exp \left[-\frac{\nu_{0n}^2 L l_e}{6R^2} \right] \\ &= 4 \sum_n \nu_{0n}^{-2} \exp \left[-\nu_{0n}^2 \left(\frac{R_G}{R} \right)^2 \right] \end{aligned} \quad (30)$$

which goes to unity in the limit $R_G/R \rightarrow 0$. In the ideal chain limit, i.e., $l_e \rightarrow l$, eq 30 is then reduced to

$$K_{\text{Casassa}} = 4 \sum_n \nu_{0n}^{-2} \exp \left[-\frac{\nu_{0n}^2 L l}{6R^2} \right] \quad (31)$$

which is identical to the result obtained by Casassa.¹¹

Figure 5 depicts the steric partition coefficients as a function of L for different values of κl . Throughout this paper, the parameter values used are $R/l = 100$, $w/l = 1$, and $w_c l = 0.1$. These values mean that we are considering the good solvent condition by $w > 0$ with the range of excluded volume interaction equal to l , and the polymer charge density is given by $\sqrt{0.1}$ elementary charge per $(l_B)^{1/2}$. As shown in Figure 5, the intramolecular interaction significantly reduces the partition coefficient compared to the Casassa's result, since $R_G^2 = Ll_e/6$ gets always much larger than $Ll/6$. For $\kappa R_G \geq 1$, the electrostatic interaction between pairs of monomers is completely screened and the polyelectrolyte conformation follows the self-avoiding walk as $R_G \sim L^{3/5}$, resulting in the partition coefficient of the self-avoiding chain (part E of Figure 5). For $\kappa R_G \leq 1$, on the other hand, the polyelectrolyte gets stretched as $R_G \sim L$ and the partition coefficient is further reduced compared to the self-avoiding chain result due to the

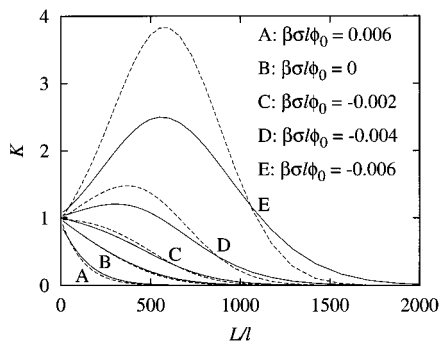


Figure 6. Partition coefficient for various values of $\beta\sigma l\phi_0$ with $\kappa R = 0$ (dashed) and with $\kappa R = 1.0$ (solid) from the perturbation theory.

manifestation of the confinement effect (parts A and B of Figure 5).

IV. Effects of the Polymer–Pore Interaction in the Weak Ionic Strength or Small Wall Potential Regime

When the pore wall is maintained with nonvanishing electrostatic potential ϕ_0 , the polymer–pore interaction may become important in determining the polymer conformation as well as the partition coefficient. In this section, we consider the wall potential in eq 12 and calculate the modified partition coefficient using the first-order perturbation theory in the regime of weak ionic strength or small wall potential.

We first examine a limiting situation of $\kappa R \rightarrow 0$, and consider the following Hamiltonian

$$\mathcal{H}_0 = -\frac{I_e}{6} \left[\frac{\partial^2}{\partial r^2} + \frac{1}{r} \frac{\partial}{\partial r} \right] + \beta\sigma\phi_0 \quad (32)$$

By solving the corresponding eigenvalue equation

$$\mathcal{H}_0\psi_{0n}^{(0)} = \lambda_{0n}^{(0)}\psi_{0n}^{(0)} \quad (33)$$

one can obtain the eigenvalues and the eigenfunctions of \mathcal{H}_0 as

$$\lambda_{0n}^{(0)} = -\frac{I_e}{6R^2} \nu_{0n}^2 + \beta\sigma\phi_0 \quad (34)$$

$$\psi_{0n}^{(0)} = \frac{1}{\pi^{1/2} R J_0(\nu_{0n})} J_0(\nu_{0n} r/R) \quad (35)$$

Here we have set the phase factor of $\psi_{0n}^{(0)}$, arising from the constant shift of \mathcal{H}_0 , equal to unity without loss of generality. From these results, the partition coefficient is obtained as

$$K = 4 \sum_n \nu_{0n}^{-2} \exp \left[-\frac{\nu_{0n}^2 L I_e}{6R^2} - \beta\sigma L\phi_0 \right] \quad (36)$$

which is shown in Figure 6 (dotted lines) for various values of $\beta\sigma l\phi_0$.

For $\beta\sigma l\phi_0 > 0$ (part A of Figure 6), K is monotonically decreasing more rapidly than the case of $\beta\sigma l\phi_0 = 0$ (part B of Figure 6), as L increases. For $\beta\sigma l\phi_0 < 0$ (parts D and E of Figure 6), however, K increases as L increases in the small L regime, while K decreases as L increases in the large L regime. It is possible to understand this

behavior by considering the limit of $\kappa R = 0$ and $L \gg 1$ as follows. In this limit, eq 14 yields $l_e \approx (Bw_c)^{2/3} L$ with $B = (4/45)(6/\pi)^{1/2}$, and the partition coefficient can be approximated as

$$K \approx 4\nu_{01}^{-2} \exp \left[-\frac{\nu_{01}^2 (Bw_c)^{2/3} L^2}{6R^2} - \beta\sigma L\phi_0 \right] \quad (37)$$

which exhibits local maxima at certain values of L for $\beta\sigma l\phi_0 < 0$. Equation 37 is therefore equivalent to the partition coefficient of a rodlike polyelectrolyte ($\kappa R_G \lesssim 1$) in the weak ionic strength limit ($\kappa R \rightarrow 0$).

To study the screening effect, we now consider the following Hamiltonian

$$\mathcal{H} = \mathcal{H}_0 + \mathcal{H}_1 \quad (38)$$

where

$$\mathcal{H}_1 = \beta\sigma\phi_0 \left[\frac{I_0(\kappa r)}{I_0(\kappa R)} - 1 \right] \quad (39)$$

In the weak ionic strength regime, i.e., $\kappa R \lesssim 1$, the potential within the pore varies smoothly and the potential depth can be small enough to treat \mathcal{H}_1 as a small perturbation. Then the set of eigenvalues $\{\lambda_{0n}\}$ and eigenfunctions $\{\psi_{0n}\}$ of \mathcal{H} can be written as

$$\lambda_{0n} = \lambda_{0n}^{(0)} + \lambda_{0n}^{(1)} \quad (40)$$

$$\psi_{0n} = \psi_{0n}^{(0)} + \psi_{0n}^{(1)} \quad (41)$$

up to the first order in \mathcal{H}_1 . Following the well-developed perturbation theory for the Schrödinger-type equation, we get the first-order corrections as

$$\begin{aligned} \lambda_{0n}^{(1)} &= \int |\psi_{0n}^{(0)}(\mathbf{r})|^2 \beta \mathcal{L}(r) \, d\mathbf{r} \\ &= 2\beta\sigma\phi_0 \int_0^1 dx x \frac{[J_0(\nu_{0n} x)]^2}{[J_0(\nu_{0n})]^2} \left[\frac{I_0(\kappa R x)}{I_0(\kappa R)} - 1 \right] \end{aligned} \quad (42)$$

and

$$\psi_{0n}^{(1)} = \sum_{k \neq n} \frac{C_{nk} \psi_{0k}^{(0)}}{\lambda_{0n}^{(0)} - \lambda_{0k}^{(0)}} \quad (43)$$

where

$$\begin{aligned} C_{nk} &= \int \psi_{0n}^{(0)}(\mathbf{r}) \beta \mathcal{L}(r) \psi_{0k}^{(0)}(\mathbf{r}) \, d\mathbf{r} \\ &= 2\beta\sigma\phi_0 \int_0^1 dx x \frac{J_0(\nu_{0n} x) J_0(\nu_{0k} x)}{J_0(\nu_{0n}) J_0(\nu_{0k})} \left[\frac{I_0(\kappa R x)}{I_0(\kappa R)} - 1 \right] \end{aligned} \quad (44)$$

Using these results, the partition coefficient can be obtained as

$$K = \sum_n \frac{2}{R^2} \int dr r' (\psi_{0n}^{(0)}(r) + \psi_{0n}^{(1)}(r)) (\psi_{0n}^{(0)}(r') + \psi_{0n}^{(1)}(r')) \exp[-L(\lambda_{0n}^{(0)} + \lambda_{0n}^{(1)})] \\ \approx 4 \sum_n \left[\left(\frac{1}{\nu_{0n}^2} + \sum_{k \neq n} \frac{C_{nk}}{\nu_{0n} \nu_{0k} (\lambda_{0n}^{(0)} - \lambda_{0k}^{(1)})} \right) \exp[-L(\lambda_{0n}^{(0)} + \lambda_{0n}^{(1)})] \right] \quad (45)$$

which is shown in Figure 6 (solid lines) for $\kappa R = 1.0$. The screening effect appears differently depending on the sign of $\beta\sigma l\phi_0$. For $\beta\sigma l\phi_0 > 0$, K is enhanced due to the screening of the repulsive wall potential, while, for $\beta\sigma l\phi_0 < 0$, K is reduced due to the screening of the attractive wall potential. For $\beta\sigma l\phi_0 = 0$, K is slightly enhanced since R_G is slightly decreased due to the screening of the monomer–monomer electrostatic interaction.

We may roughly estimate the validity regime of our perturbation theory as follows. When $\kappa R \gg 1$, the dimensionless potential depth for the whole chain goes such as $\beta\sigma L\phi_0$, which yields the condition

$$|\beta\sigma L\phi_0| \ll \frac{Ll_e}{R^2} \quad (46)$$

for our perturbation theory to be valid. When $\kappa R \lesssim 1$, on the other hand, the condition is changed to

$$|\beta\sigma L\phi_0|(\kappa R)^2 \ll \frac{Ll_e}{R^2} \quad (47)$$

since the potential depth is reduced by the factor of $(\kappa R)^2$. This means that our perturbation theory may be valid even for large values of $|\beta\sigma L\phi_0|$, provided that $\kappa R \ll 1$. In addition, for sufficiently large values of L , our perturbation theory is expected to be valid for any value of $|\beta\sigma L\phi_0|$, since l_e is an increasing function of L and the “kinetic energy” prevails over the potential energy. In this study, we treated the ionic solution using the Debye–Hückel approximation and neglected the effects arising from the entropy loss of counterions. The counterion effect could play an important role in experiments, in particular, in the weak ionic strength regime, and care should be taken for the application of our results in this section.

V. Effects of the Polymer–Pore Interaction in the Strong Ionic Strength Regime

For $\kappa R \geq 1$, the polymer can be localized near the pore center or near the wall when the polymer–pore interaction is strongly repulsive or strongly attractive, respectively. One may then expect that the associated set of eigenvalues of the Hamiltonian exhibits a well-separated discrete spectrum, so that the lowest eigenvalue mode dominates the others. In view of this, we use the ground state dominance approximation

$$G_L(\mathbf{r}, \mathbf{r}') \simeq e^{-L\lambda_0} \psi_0(\mathbf{r}) \psi_0(\mathbf{r}') \quad (48)$$

and follow the standard variational scheme to approximately estimate the partition coefficient. To this end, we choose a trial ground-state eigenfunction as

$$\Psi_0(r) = A \left[1 - \left(\frac{r}{R} \right)^2 \right] \exp \left[\alpha \left(\frac{r}{R} \right)^2 \right] \quad (49)$$

where α is a variational parameter to be determined later, and A is given by

$$A^2 = \left(\frac{1}{R^2} \right) \frac{8\alpha^3}{e^{2\alpha} - 2\alpha^2 - 2\alpha - 1} \quad (50)$$

from the normalization condition

$$\int_0^R |\Psi_0(r)|^2 r dr = 1 \quad (51)$$

The trial function is chosen to satisfy the following boundary conditions:

$$\left. \frac{\partial \Psi_0(r)}{\partial r} \right|_{r=0} = 0 \quad (52)$$

$$\Psi_0(r=R) = 0 \quad (53)$$

Using the ground-state dominance approximation, the monomer density distribution in eq 25 is reduced to

$$\rho(r) = |\Psi_0(r)|^2 \quad (54)$$

and the probability density of finding a monomer with its radial position at r is given by

$$P(r) = r\rho(r) = r|\Psi_0(r)|^2 \quad (55)$$

Figure 7 depicts $P(r)$ for different values of α , where one can see that the distribution is localized near the pore center or near the wall as α decreases or increases, respectively.

Using the trial function, we get the variational ground-state eigenvalue as a function of the parameter α as

$$\lambda_0(\alpha) = \int_0^R \Psi_0(r) \left[-\frac{l_e}{6} \left(\frac{\partial^2}{\partial r^2} + \frac{1}{r} \frac{\partial}{\partial r} \right) + \beta\sigma\phi_0 \frac{I_0(\kappa r)}{I_0(\kappa R)} \right] \Psi_0(r) r dr \\ = -\frac{l_e A^2}{6} \left[\frac{(1 - 2\alpha)e^{2\alpha} - 1}{4\alpha^2} - \frac{1}{2} \right] + \frac{A^2 R^2 \beta\sigma\phi_0}{I_0(\kappa R)} \int_0^1 dx x(1 - x^2)^2 e^{2\alpha x^2} I_0(\kappa R x) \quad (56)$$

To minimize $\lambda_0(\alpha)$ with respect to α , we require

$$\left. \frac{\partial \lambda_0(\alpha)}{\partial \alpha} \right|_{\alpha=\alpha_0} = 0 \quad (57)$$

which we will solve numerically. Once we determine α_0 in terms of given parameters, the partition coefficient can be obtained as

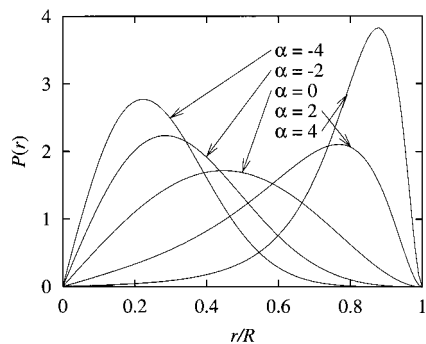


Figure 7. Variational monomer density distribution for different values of the variational parameter α .

$$\begin{aligned}
 K &= \left(\frac{2}{R^2}\right) \int_0^R dr r \int_0^R dr' r' e^{-L\phi_0} \Psi_0(r) \Psi_0(r') \\
 &= e^{-L\phi_0} \left(\frac{2}{R^2}\right) \left[\int_0^R dr r \Psi_0(r)\right]^2 \\
 &= \frac{A^2 R^2}{2\alpha_0^4} (e^{\alpha_0} - 1 - \alpha_0)^2 e^{-L\phi_0(\alpha_0)} \quad (58)
 \end{aligned}$$

The partition coefficients for $\beta\sigma l\phi_0 = +0.01$ and -0.01 are shown in Figures 8 and 9 (solid lines), respectively. For comparisons, we also present the results from our perturbation theory for the same parameters (dotted lines), which are in good agreements with those of the variational theory, especially for large values of L , as will be discussed below.

For the case of strongly repulsive polymer–pore interaction, the partition coefficient is shown in Figure 8 for various values of κR . As L increases, K monotonically decreases as expected, and, as κR increases, K increases due to the enhanced screening of the repulsive interaction. For $\kappa R \geq 1$, the polymer–pore interaction becomes a finite-ranged repulsive one, and consequently the monomer distribution is localized near the pore center. In the extreme case of $\kappa R \gg 1$, K should follow the steric partition coefficient since the polymer–pore interaction is completely screened. Likewise, for large enough values of L , the monomer distribution is no longer localized due to the intramolecular interactions, again yielding the steric partitioning behavior.

When the polymer–pore interaction is strongly attractive, on the other hand, the partition coefficient strongly depends on the value of κR as shown in Figure 9. The larger the value of κR , the more screening of the polymer–pore attractive interaction occurs, yielding smaller partition coefficients. In the extreme case of $\kappa R \gg 1$, the attraction is completely screened and K should follow the steric partitioning behavior. For $\kappa R \geq 1$, the polyelectrolyte adsorbs to the pore wall and K increases as L increases in the small L regime. However, for large values of L , the monomer distribution is no longer localized near the wall due to the repulsion between monomers, following the steric partitioning behavior as in the case of the strongly repulsive interaction. This is why our perturbation theory remains valid, irrespective of the polymer–pore interaction characteristics, only if L is sufficiently large so that the intramolecular interactions mainly govern the monomer density distribution.

VI. Summary

The polyelectrolyte partitioning into a pore is basically a phenomenon of interplay or competition between steric

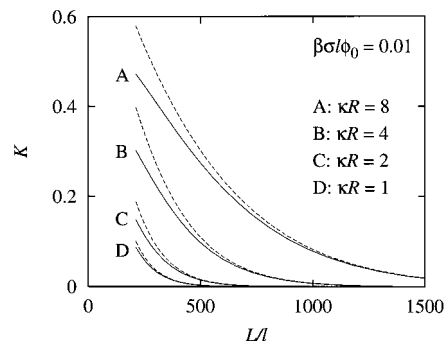


Figure 8. Partition coefficient with a strongly repulsive pore wall ($\beta\sigma l\phi_0 = 0.01$), calculated from variational theory (solid) and perturbation theory (dashed).

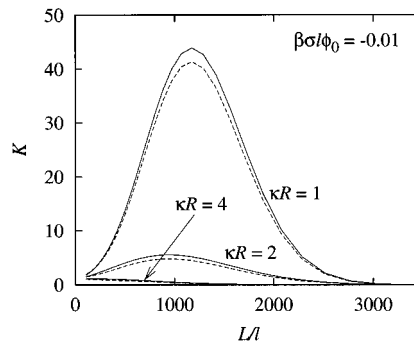


Figure 9. Partition coefficient with a strongly attractive pore wall ($\beta\sigma l\phi_0 = -0.01$), calculated from variational theory (solid) and perturbation theory (dashed).

and electrostatic polymer–pore interactions, depending upon the ionic strength of surrounding fluids. When the electrostatic interaction is repulsive, it adds to the steric interaction and the polymer can hardly be inserted into the pore. For the case of attractive electrostatic interaction, on the other hand, the steric interaction competes with it, and the partition coefficient can exhibit local maxima as the polymer size changes. In this study, we have shown how the partitioning behavior is modified due to the intramolecular interactions. The electrostatic interaction between monomers adds to the excluded volume interaction, which determines the polymer conformation depending upon the ionic strength. The polymer size, determined by the intramolecular interaction, turns out to be a crucial factor in the partitioning of polyelectrolytes just as the particle size is a key parameter in the partitioning of colloids.

In the presence of ionic solutions, there appears a new relevant length scale κ^{-1} , the Debye screening length, in addition to the pore size R and the polymer size R_G . The polyelectrolyte partitioning can be understood in terms of these three length scales. When $R_G \ll R$ and $R_G \ll \kappa^{-1}$, the polyelectrolyte can be considered as a colloidal particle and the partitioning behavior follows that of a charged particle. In the limit of $\kappa = 0$, for any value of R and R_G , the electrostatic potential within the pore has a constant value and the constant-shifted free energy determines the partitioning behavior. When $\kappa R \leq 1$, the electrostatic potential within the pore smoothly varies, and our perturbation theory works as a good approximation to examine the screening effect for any value of R_G . For $R \geq R_G \geq \kappa^{-1}$, finally, the polyelectrolyte gets localized near the wall or near the pore center depending upon the sign of the wall potential. In this regime, the polymer–pore interaction mainly governs the partitioning behavior, where our variational theory

proves to be a good approximation. It should be pointed out that both the perturbation theory and the variational theory give the same result for a very long chain, irrespective of the polymer–pore interaction parameters, since the intramolecular interaction mainly determines the monomer density distribution. This signifies that the intramolecular interaction is as much important as the polymer–pore interaction in determining the partitioning behavior.

Regarding the excluded volume effects and the chain stiffness, currently known results from experiments and computer simulations are in reasonable agreements with theoretical predictions.¹ To our knowledge, however, effects of electrostatic interactions have not been explored experimentally in the partitioning of polymers. Lin and Deen examined theoretically the effects of various long-range polymer–pore interactions,⁴ yet their predictions remain to be confirmed. It would be interesting to verify experimentally their results as well as the effects of intramolecular electrostatic interactions examined in this paper.

Acknowledgment. The authors gratefully acknowledge the basic research fund provided to M.-S.C. by KIST (1999).

References and Notes

- (1) Teraoka, I. *Prog. Polym. Sci.* **1996**, *21*, 89.
- (2) Doi, M.; Edwards, S. F. *The Theory of Polymer Dynamics*; Clarendon Press: Oxford, England, 1986.
- (3) Davidson, M. G.; Suter, U. W.; Deen, W. M. *Macromolecules* **1987**, *20*, 1141.
- (4) Lin, N. P.; Deen, W. M. *Macromolecules* **1990**, *23*, 2947.
- (5) Park, P. J.; Sung, W. *J. Chem. Phys.* **1999**, *111*, 5259.
- (6) Hoagland, D. A.; Muthukumar, M. *Macromolecules* **1992**, *25*, 6696.
- (7) Deen, W. M. *AIChE J.* **1987**, *33*, 1409.
- (8) Davidson, M. G.; Deen, W. M. *J. Membr. Sci.* **1988**, *35*, 167.
- (9) Muthukumar, M.; Baumgärtner, A. *Macromolecules* **1989**, *22*, 1937.
- (10) Chun, M.-S.; Phillips, R. J. *AIChE J.* **1997**, *43*, 1194.
- (11) Casassa, E. F. *J. Polym. Sci. B* **1967**, *5*, 773.
- (12) Daoud, M.; de Gennes, P. G. *J. Phys. (Paris)* **1977**, *38*, 85.
- (13) Borukhov, I.; Andelman, D.; Orland, H. *Europhys. Lett.* **1995**, *32*, 499.
- (14) Satterfield, C. N.; Colton, C. K.; de Turckheim, B.; Copeland, T. M. *AIChE J.* **1978**, *24*, 937.
- (15) Liu, L.; Li, P.; Asher, S. A. *Nature* **1999**, *397*, 141.
- (16) Bezrukov, S. M.; Vodyanoy, I.; Brutyan, R. A.; Kasianowicz, J. J. *Macromolecules* **1996**, *29*, 8517.
- (17) Muthukumar, M. *J. Chem. Phys.* **1987**, *86*, 7230.
- (18) von Goeler, F.; Muthukumar, M. *J. Chem. Phys.* **1994**, *100*, 7796.

MA000004O